Commun. Theor. Phys. (Beijing, China) **47** (2007) pp. 741–746

Vol. 47, No. 4, April 15, 2007

Magnetic Properties of a Mixed Spin-2 and Spin-5/2 Heisenberg Ferrimagnetic System on a Two-Dimensional Honeycomb Lattice: Green's Function Approach*

YAO Kai-Lun,[1,2] LI Jian-Wen,[1] LIU Zu-Li,[1] FU Hua-Hua,[1] and ZU Lin[1]

[1]Department of Physics, Huazhong University of Science and Technology, Wuhan 430074, China

[2]International Center of Material Physics, the Chinese Academy of Sciences, Shenyang 110015, China

(Received April 30, 2006)

Abstract *The multisublattice Green's function technique is applied to study the magnetic properties of a mixed spin-2 and spin-5/2 Heisenberg ferrimagnetic system on a two-dimensional honeycomb lattice. The role of the different interactions in the Hamiltonian is explored. When only the nearest-neighbor interaction and the single-ion anisotropy are included, our results indicate that there are compensation points at finite temperatures. When the next-nearest-neighbor interaction exceeds a minimum value that depends on the other parameters in the Hamiltonian, the compensation point disappears. The next-nearest-neighbor interaction has the effect of changing the compensation temperature.*

PACS numbers: 75.10.Jm, 75.40.Gb, 75.50.Gg
Key words: Heisenberg ferrimagnetic, Green function, spin-wave spectra, magnetization, critical temperature, compensation temperature

1 Introduction

Recently many experimental studies have accumulated in the area of molecular-based magnetic materials, and the magnetic properties become an important focus of scientific interest.[1−5] Among these materials, a number of bimetallic molecular-based magnetic materials, in which two kinds of magnetic atoms alternate regularly, exhibit ferrimagnetic properties and seem to play an important role. One example is the recently developed amorphous $V(TCNE)_{x\cdot y}$ order ferrimagnetically as high as 400 K.[6,7] Another experimental group synthesized compounds such as $AM^{II}Fe^{III}(C_2O_4)_3$ (A=N(n-$C_nH_{2n+1})_4$, $n = 3 \sim 5$, M^{II} = Mn, Fe),[8] which have critical temperatures between 35 and 48 K, and some of them have compensation temperatures near 30 K, depending on the kind of a cation A^+. The compensation temperature is the temperature where the resultant magnetization vanishes below the critical temperature. The behavior at the compensation point is of fundamental significance in the field of thermomagnetic recording.

Theoretically, mixed Ising systems have been used to describe the above materials by several methods such as the mean-field theory,[9] the effective-field theory,[10] the cluster variational theory,[11] and so on. In mixed Ising model, the spins are scalar quantity. Actually, the spins should be vectors in the ferrimagnetic compounds $AM^{II}Fe^{III}(C_2O_4)_3$ (A = N(n-$C_nH_{2n+1})_4$, $n = 3 \sim 5$, M^{II} = Mn, Fe). The magnetic properties of the system may be affected by the quantum fluctuation of spins. So, we will study a mixed spin-5/2 and spin-2 quantum Heisenberg system on a two-dimensional honeycomb lattice with the multisublattice Green-function technique in order to investigate the effects of the nearest-neighbor and next-nearest-neighbor interactions between spins on the magnetic properties. The similar method have been applied to the mixed spin-3/2 and spin-1/2 Heisenberg ferrimagnetic system on a square lattice.[12] We compare our theoretical studies with the results obtained by the mean-field approximation (MFA) and the effective-field theory (EFT). It can be found that our results are consistent with experimental results. This paper is organized as follows. The model and the fundamental equations are presented in Sec. 2. In Sec. 3, the spin-wave spectrum of the ground state, the numerical results of the total magnetizations in the whole range of temperatures and the finite-temperature phase diagram are given. We finally present the conclusions in Sec. 4.

2 Model and Green's Function Method

We study a layered honeycomb lattice with spin-2 and spin-5/2 spins, which represent Fe^{II} and Fe^{III} atoms, respectively. Both spins locate in alternating sites of a two-dimensional honeycomb lattice and the lattice has a layered structure, as shown in Fig. 1. The Hamiltonian we adopt is given by

$$H = 2J \sum_{\langle nn \rangle} s_{ai} s_{bj} - J_1 \sum_{\langle nnn \rangle} s_{ai} s_{ai'} - J_2 \sum_{\langle nnn \rangle} s_{bj} s_{bj'} - D_1 \sum_i (s_{ai}^z)^2 - D_2 \sum_j (s_{bj}^z)^2 , \quad (1)$$

where $\langle nn \rangle$ and $\langle nnn \rangle$ stand for the nearest- and next-nearest-neighbors, respectively. i, i' belong to the sublattice A (spin-2), j, j' belong to the sublattice B (spin-5/2). J is the antiferromagnetic nearest-neighbor exchange interaction,

*The project supported by National Natural Science Foundation of China under Grant Nos. 10574048 and 20490210

J_1 and J_2 are the ferromagnetic next-nearest-neighbor interactions between spins in sublattice A and B, respectively. D_1 and D_2 are the single-ion anisotropy of sublattice A and sublattice B, respectively.

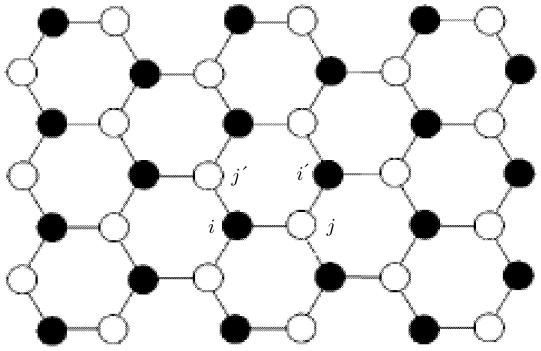

Fig. 1 The honeycomb layer with periodic boundary condition. The filled and open circles are Fe^{II} and Fe^{III}.

We will begin with the formalism of the two-time Green's function whose time-Fourier transform satisfies the equation

$$\omega\langle\langle A;B\rangle\rangle = (2\pi)^{-1}\langle\,[A,B]\,\rangle + \langle\langle\,[A,H];B\rangle\rangle\,, \tag{2}$$

where $\langle BA\rangle$ is defined by

$$\langle BA\rangle = \mathrm{i}\int_{-\infty}^{+\infty}\mathrm{d}\omega\,\{\langle\langle A;B\rangle\rangle_{\omega+\mathrm{i}\delta} - \langle\langle A;B\rangle\rangle_{\omega-\mathrm{i}\delta}\}n(\omega/k_BT)\,, \tag{3}$$

where $n(x) = [\exp(x)-1]^{-1}$ and k_B is the Boltzmann constant. We consider the Green function $\langle\langle S^+_{ai};S^-_{al}\rangle\rangle$ and $\langle\langle S^+_{bj};S^-_{al}\rangle\rangle$ using the formalism (2), we get

$$\begin{aligned}\omega\langle\langle S^+_{ai};S^-_{al}\rangle\rangle &= \frac{\langle S^z_{ai}\rangle}{\pi}\delta_{aial} + 2J\Big\langle\Big\langle\Big(-\sum_{\langle nn\rangle}S^z_{bj}S^+_{ai} + \sum_{\langle nn\rangle}S^+_{bj}S^z_{ai}\Big);S^-_{al}\Big\rangle\Big\rangle \\ &\quad - J_1\Big\langle\Big\langle\Big(-\sum_{\langle nnn\rangle}S^z_{ai'}S^+_{ai} + \sum_{\langle nnn\rangle}S^+_{ai'}S^z_{ai}\Big);S^-_{al}\Big\rangle\Big\rangle + D_1\langle\langle(S^z_{ai}S^+_{ai}+S^+_{ai}S^z_{ai});S^-_{al}\rangle\rangle\,, \end{aligned}\tag{4}$$

$$\begin{aligned}\omega\langle\langle S^+_{bj};S^-_{al}\rangle\rangle &= 2J\Big\langle\Big\langle\Big(-\sum_{\langle nn\rangle}S^z_{ai}S^+_{bj} + \sum_{\langle nn\rangle}S^+_{ai}S^z_{bj}\Big);S^-_{al}\Big\rangle\Big\rangle\,. \\ &\quad - J_2\Big\langle\Big\langle\Big(-\sum_{\langle nnn\rangle}S^z_{bj'}S^+_{bj} + \sum_{\langle nnn\rangle}S^+_{bj'}S^z_{bj}\Big);S^-_{al}\Big\rangle\Big\rangle + D_2\langle\langle(S^z_{bj}S^+_{bj}+S^+_{bj}S^z_{bj});S^-_{al}\rangle\rangle\,. \end{aligned}\tag{5}$$

We decouple the Green's function on the right-hand side of the equations as follows. The Green functions coming from the exchange term such as $\langle\langle S^+_{bj}S^z_{ai} - S^z_{bj}S^+_{ai};S^-_{al}\rangle\rangle$ are decoupled by using the random phase approximation (RPA),[13] for example

$$\langle\langle S^+_{bj}S^z_{ai};S^-_{al}\rangle\rangle \to \langle S^z_{ai}\rangle\langle\langle S^+_{bj};S^-_{al}\rangle\rangle\,. \tag{6}$$

The Green functions coming from the single-ion anisotropy term such as $\langle\langle(S^z_{ai}S^+_{ai}+S^+_{ai}S^z_{ai});S^-_{al}\rangle\rangle$ cannot be treated by RPA because we no longer separate the longitudinal and transversal components of spin operator at the same site from each other, and are coupled by using the Anderson and Callen's decoupling scheme,[14] for example

$$\langle\langle(S^z_{ai}S^+_{ai}+S^+_{ai}S^z_{ai});S^-_{al}\rangle\rangle \to t_a\langle\langle S^+_{ai};S^-_{al}\rangle\rangle\,, \tag{7}$$

where

$$t_a = \Big\{1 - \frac{1}{S_a^2}\left[S_a - \langle(S^z_a)^2\rangle\right]\Big\}\langle S^z_a\rangle\,. \tag{8}$$

This decoupling scheme gives reasonable results[15] and does not make the theory very complicated.

From Eqs. (4) and (5), we can get the Green's function as follows:

$$G_a(k,\omega) = \frac{m_a}{\pi P_k}\Big[\frac{E^+ + A_2}{\omega - E^+} - \frac{E^- + A_2}{\omega - E^-}\Big]\,, \tag{9}$$

where

$$m_a = \langle S^z_{ai}\rangle, \qquad m_b = \langle S^z_{bj}\rangle, \quad E^\pm = \frac{1}{2}\left[-\left(A_0 + A_2\right) \pm P_k\right]\,, \tag{10}$$

$$A_0 = 6Jm_b - 6J_1m_a - D_1t_a + 2J_1m_a\left[\cos\left(\sqrt{3}k_xa\right) + 2\cos\Big(\frac{\sqrt{3}}{2}k_xa\Big)\cos\Big(\frac{3}{2}k_ya\Big)\right], \tag{11}$$

$$A_1 = -2Jm_a\left[\mathrm{e}^{\mathrm{i}k_ya} + 2\cos\Big(\frac{\sqrt{3}}{2}k_xa\Big)\mathrm{e}^{-\mathrm{i}k_ya/2}\right], \tag{12}$$

$$A_2 = 6Jm_a - 6J_2m_b - D_2t_b + 2J_2m_b\left[\cos\left(\sqrt{3}k_xa\right) + 2\cos\Big(\frac{\sqrt{3}}{2}k_xa\Big)\cos\Big(\frac{3}{2}k_ya\Big)\right], \tag{13}$$

$$A_3 = -2Jm_b\left[\mathrm{e}^{-\mathrm{i}k_ya} + 2\cos\Big(\frac{\sqrt{3}}{2}k_xa\Big)\mathrm{e}^{\mathrm{i}k_ya/2}\right], \tag{14}$$

$$P_k^2 = (A_0 - A_2)^2 + 4A_1A_3\,. \tag{15}$$

Similarly, the Green's function $G_b(k,\omega)$ can be found

$$G_b(k,\omega) = \frac{m_b}{\pi P_k}\Big[\frac{E^+ + A_0}{\omega - E^+} - \frac{E^- + A_0}{\omega - E^-}\Big]. \tag{16}$$

Then the sublattice magnetization m_a and m_b are easily obtained from the spectral theorem and given by

$$m_a = \frac{(S_a - \Phi_a)(1+\Phi_a)^{2S_a+1} + (1 + S_a + \Phi_a)\Phi_a^{2S_a+1}}{(1+\Phi_a)^{2S_a+1} - \Phi_a^{2S_a+1}}, \tag{17}$$

$$m_b = \frac{(S_b - \Phi_b)(1+\Phi_b)^{2S_b+1} + (1 + S_b + \Phi_b)\Phi_b^{2S_b+1}}{(1+\Phi_b)^{2S_b+1} - \Phi_b^{2S_b+1}}, \tag{18}$$

$$\langle (S_a^z)^2\rangle = S_a(S_a+1) - (1+2\Phi_a)m_a\,, \tag{19}$$

$$\langle (S_b^z)^2\rangle = S_b(S_b+1) - (1+2\Phi_b)m_b\,, \tag{20}$$

where

$$\Phi_a = \frac{2}{N}\sum_k \frac{1}{P_k}\left[\big(E^+ + A_2\big)\,n\Big(\frac{E^+}{k_BT}\Big) - \big(E^- + A_2\big)\,n\Big(\frac{E^-}{k_BT}\Big)\right], \tag{21}$$

$$\Phi_b = \frac{2}{N}\sum_k \frac{1}{P_k}\left[\big(E^+ + A_0\big)\,n\Big(\frac{E^+}{k_BT}\Big) - \big(E^- + A_0\big)\,n\Big(\frac{E^-}{k_BT}\Big)\right]. \tag{22}$$

And the total magnetization of the system is given by

$$\langle S^z\rangle = m_a + m_b\,. \tag{23}$$

Equations (17) $\sim$ (20) form a set of self-consistent equations which can be solved numerically.

3 Results and Discussion

Firstly, let us study the characteristic properties of the ground state. The spin-wave spectra of the ground state for several values of J_2/J are shown in Fig. 2, from which we can see that there are two branches of the spin wave. E^+ is the acoustic branch and E^- is the optical branch when the anisotropies D_1 and D_2 are equal to zero. When the anisotropy D_1 and D_2 are not equal to zero, both branches of spin-wave spectrum are optical branches and an energy gap appears, which is just the effect of the anisotropies. In both cases, the branch of spin-wave spectrum E^- is always negative. The negative energy can be understood in the following manner. As elementary excitations, we consider the magnon vacuum as the ground state. Therefore, magnons excited out of the filled sea constitute the branches with energies E^+ and E^-. It is quite obvious that the positive energy E^+ is sensitive to the change of the next-nearest-neighbor interaction J_2 as J_1 is zero, whereas the negative energy branch E^- is insensitive to the change of J_2. Each figure shows that E^+ increases as J_2 grows.

Now, let us turn our attention to the magnetic behavior in the whole range of temperatures. In Figs. 3 and 4, we show how the next-nearest-neighbor interaction J_2 affects the total magnetization, selecting the next-nearest-neighbor interaction $J_1/J = 0.0$. Figure 3(a) is plotted with $D_1/J = D_2/J = 4.0$. It is clearly indicated that there is no compensation point. As for the type of magnetization curves, we can see two types of behavior. When only the nearest-neighbor interaction is included, the magnetization curves behave as Q-type, and behave as P-type when the next-nearest-neighbor interaction J_2 is taken into account in the Neel's classification.[16] From Fig. 3(b) we can see that only the P-type magnetization curves exist when $D_1/J = 0.0$, $D_2/J = 4.0$, nevertheless the total magnetization is more sensitive to the change of J_2/J than that in Fig. 3(a). It is more interesting that compensation points appear when only the nearest-neighbor interaction is included for $D_1/J = 8.0$, $D_2/J = 0.0$, as is shown in Fig. 4. Notice that

our results are similar to ones obtained through the effective-field theory and the mean-field approximation for the Ising model.[17] In addition, figure 4 also indicates that the compensation point moves towards right with the increasing of J_2/J, but the compensation point disappears as J_2/J exceeds the critical value $J_{2C}/J = 0.674$. It can be seen from Figs. 3 and 4 that our results are consistent with the experiment.[8,18] We explain it as follows. The kind of an organic cation A^+ has a great influence on the interactions between different spins, especially on the next-nearest-neighbor interactions. As a result, some of the ferrimagnetic compounds $AM^{II}Fe^{III}(C_2O_4)_3$ have compensation temperatures, others have not.

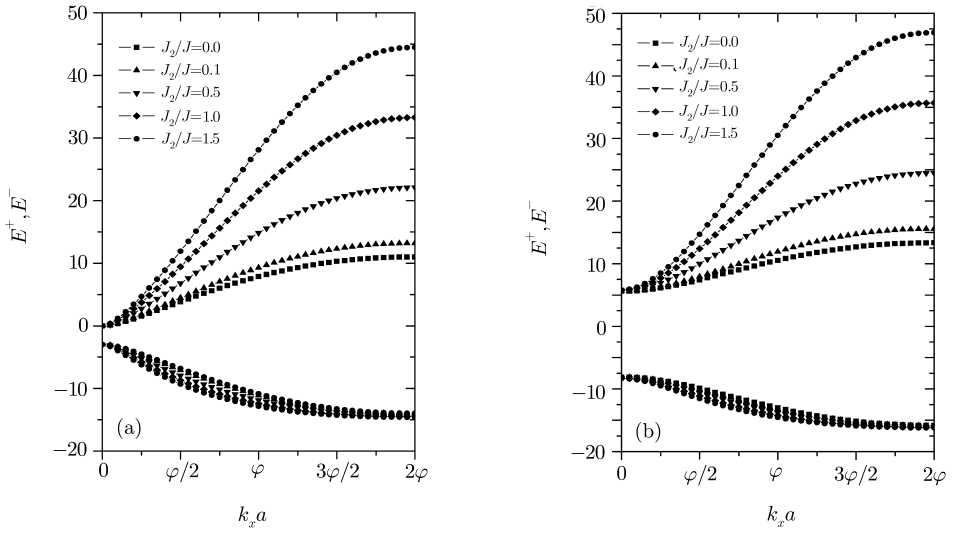

Fig. 2 The spin-wave spectra of the ground state along the k_x-axis in the first Brillouin region with $J_1/J = 0.0$ for different values of J_2/J. (a) $D_1/J = D_2/J = 0$, (b) $D_1/J = D_2/J = 0.5$ ($\varphi = 2\sqrt{3}\pi/9$).

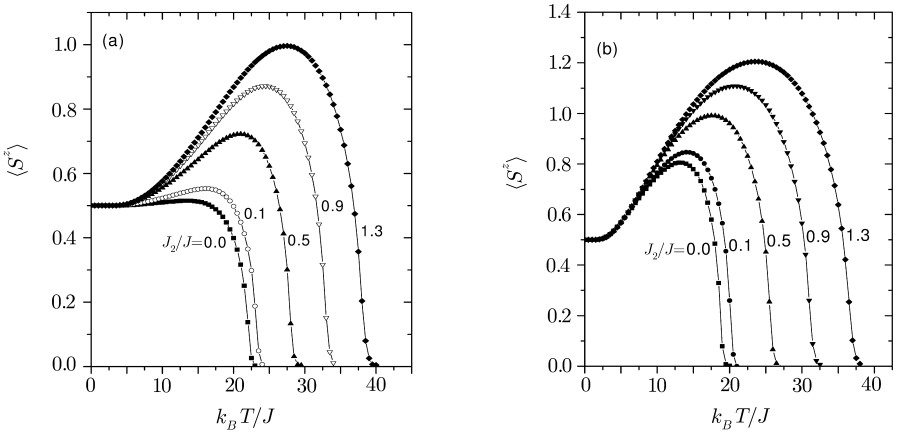

Fig. 3 Temperature dependence of the total magnetization for several values of J_2/J when $J_1/J = 0.0$. Numbers next to curves are values of J_2/J. (a) $D_1/J = D_2/J = 4.0$. (b) $D_1/J = 0.0$, $D_2/J = 3.0$.

The phase diagram of the compensation and critical temperature vs. D_1/J for several values of J_2/J with $J_1/J = D_2/J = 0.0$ is shown in Fig. 5. The critical temperature is the temperature where the total magnetization and the sublattice magnetizations all vanish. We can determine the compensation and critical temperature from the self-consistent equations (17) $\sim$ (20). As one can see from Fig. 5, each curve of critical temperature intersects with the corresponding curve of compensation temperature, which is labeled the same value of J_2/J as the corresponding curve of critical temperature. The critical temperature T_c increases and the compensation temperature $T_{\rm comp}$ decreases with the increasing of D_1. It is also worthy of notice that both T_c and $T_{\rm comp}$ increase with the increasing of J_2, meanwhile the cross point moves towards right. In the inset are the theoretical results by means of the effective-field theory and the mean-field approximation for the Ising model from Ref. [17]. It can be found that our results are similar to ones based on the two theoretical methods. The critical value D_{1C}/J we obtained is 2.625, while $D_{1C}/J = 2.934$ for the

MFA and $D_{1C}/J = 3.349$ for the EFT.

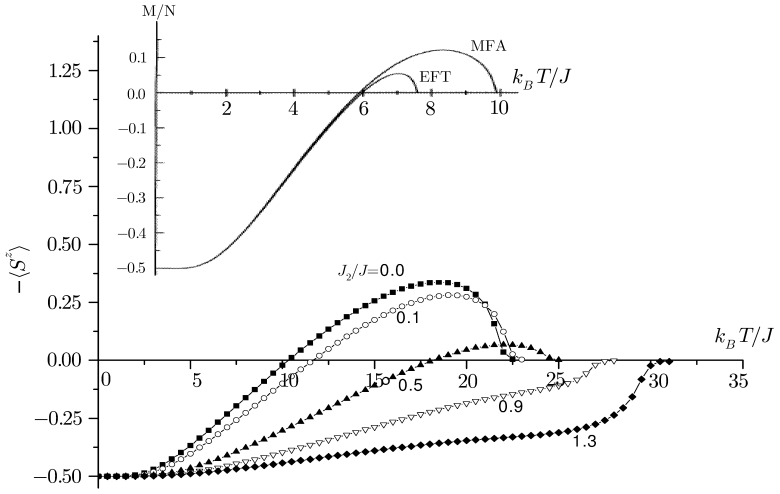

Fig. 4 Temperature dependence of the total magnetization for several values of J_2/J when $J_1/J = 0.0$, $D_1/J = 8.0$, $D_2/J = 0.0$. Numbers next to curves are values of J_2/J. In the inset is the theoretical results for $J_2/J = 0.0$ from Ref. [17].

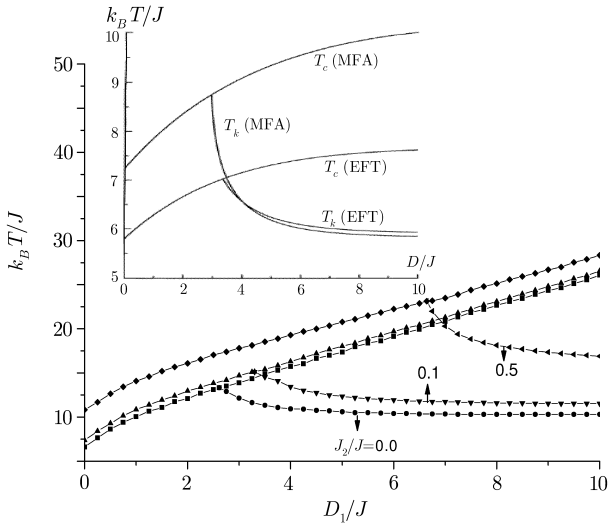

Fig. 5 Critical and compensation temperatures as function of D_1/J when $J_1/J = 0.0$, $D_2/J = 0.0$. Numbers next to curves are values of J_2/J. In the inset is the theoretical results for $J_2/J = 0.0$ from Ref. [17].

Figure 6(a) shows the phase diagram of the compensation and critical temperature vs. J_1/J for several values of D_2/J as $J_2/J = 0.2$ and $D_1/J = 0.5$. It can be seen from Fig. 6(a) that the value of J_1/J which corresponds to the intersection point is the critical value J_{1C}/J. The mixed spin-2 and spin-5/2 ferrimagnetic Heisenberg system on a two-dimensional honeycomb lattice exhibits only one compensation point below the critical temperature when the value of J_1/J is larger than a critical value J_{1C}/J. Obviously when J_1/J is smaller than a critical value J_{1C}/J, the system does not have a compensation temperature. From Fig. 6(a) we can also see that the larger D_2 is, the larger J_1/J is. It should be pointed out that, for fixed value of D_2/J, the critical temperature increases sharply and compensation temperature decreases with the increasing of J_1/J. On the other hand, the critical and compensation temperature become higher with the increasing of D_2/J when J_1/J is fixed. Finally, Figure 6(b) shows the phase diagram of the compensation and critical temperature vs. J_1/J for several values of J_2/J as $D_1/J = 0.5$, $D_2/J = 0.5$, the situation is very similar to that in Fig. 6(a). We can analyze the above phenomena as follows: when $T = 0$ K, the magnetization of the Fe^{III} sublattice is 5/2 and the magnetization of Fe^{II} sublattice is 2, as the temperature increases the magnetization of Fe^{II} sublattice decreases more slowly than that of Fe^{III} sublattice because the total magnetization is zero at the compensation point. As a result, the larger the next-nearest-neighbor interaction J_1/J is, the smaller

the compensation temperature $T_{\rm comp}$ is. The larger the single-ion anisotropy D_1/J is, the larger the compensation temperature is. The situation is the same as J_2/J and D_2/J.

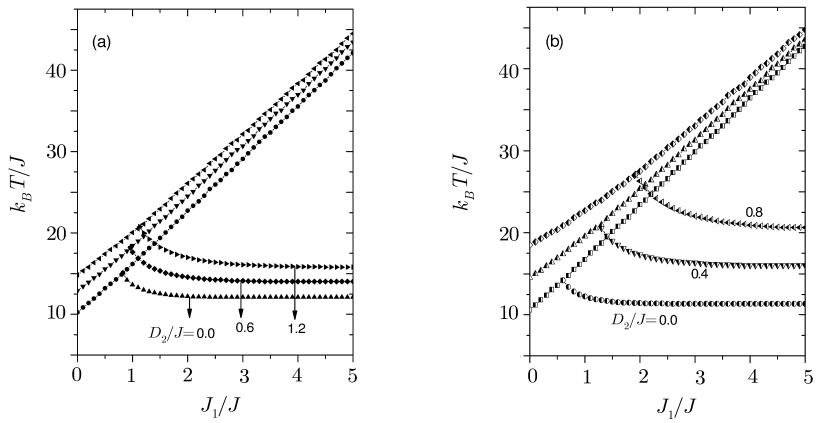

Fig. 6 Critical and compensation temperatures as function of J_1/J. (a) $J_2/J = 0.2$, $D_1/J = 0.5$. Numbers next to curves are values of D_2/J. (b) $D_1/J = D_2/J = 0.5$. Numbers next to curves are values of J_2/J.

4 Conclusion

We have applied Green's function method to study a mixed spin-2 and spin-5/2 Heisenberg ferrimagnetic system on a two-dimensional honeycomb lattice. The Hamiltonian includes nearest-, next-nearest-neighbors interactions and the single-ion anisotropy. The spin-wave spectra of the ground state, the sublattice magnetizations and the phase diagram showing the critical and compensation temperature are obtained. Our study indicates that both the next-nearest-neighbor interactions and the single-ion anisotropy have a great effect on the phase diagram.

Finally, one should notice that compensation temperatures are extremely dependent on the interactions in the Hamiltonian and that there is a relatively narrow combination of parameters for which they can exist. Experimental evidence of the effect of long-range interactions on compensation points has already been found.[19,20]

References

[1] K. Inoue, F. Iwahori, A.S. Markosyan, and H. Iwamura, Coordination Chemistry Reviews **198** (2000) 219.
[2] K. Maekawa, D. Shiomi, T. Ise, K. Sato, and T. Takui, J. Phys. Chem. B **109** (2005) 3303.
[3] C.D. Smith, S.E. Bottle, P.C. Junk, *et al.*, Synthetic Metals **138** (2003) 501.
[4] T. Sugano, S.J. Blundell, W. Hayes, and P. Day, Synthetic Metals **121** (2001) 1812.
[5] K. Hayakawa, D. Shiomi, T. Ise, K. Sato, and T. Takui, J. Phys. Chem. B **109** (2005) 9195.
[6] J.M. Manriquez, G.T. Yee, R.S. McLean, A.J. Epstein, and J.S. Miller, Science **252** (1991) 1415.
[7] A. Ganeschi and D. Gatteschi, Prog. Inorg. Chem. **37** (1991) 331.
[8] C. Mathonière, C.J. Nuttall, S.G. Carling, and P. Day, Inorg. Chem. **35** (1996) 1201.
[9] T. Kaneyoshi and J.C. Chen, J. Magn. Magn. Mater. **98** (1991) 201.
[10] T. Kaneyoshi, Solid State Commun. **70** (1989) 975.
[11] J.W. Tucker, J. Magn. Magn. Mater. **195** (1999) 733.
[12] Jun Li, Guo-Zhu Wei, and An DU, J. Magn. Magn. Mater. **269** (2004) 410.
[13] R.A. Tahir-Kheli and D. ter Haar, Phys. Rev. **127** (1962) 88.
[14] F.B. Anderson and H.B. Callen, Phys. Rev. **136** (1964) A1068.
[15] J.F. Devlin, Phys. Rev. B **4** (1971) 136.
[16] L. Néel, Ann. Phys. Paris **3** (1948) 137.
[17] T. Kaneyoshi, Y. Nakamura, and S. Shin, J. Phys.: Condens. Matter **10** (1998) 7025.
[18] S.G. Carling, P. Day, and C.J. Nuttall, Spectrochimica Acta Part A **57** (2001) 1971.
[19] Eric E. Fullerton, J.S. Jiang, Christine Rehm, *et al.*, Appl. Phys. Lett. **71** (1997) 1579.
[20] L. Ertl, G. Endl, and H. Hoffmann, J. Magn. Magn. Mater. **113** (1992) 227.